with a lesser degree of certainty for several bands in both spectra, due primarily to poorer computed relative intensities. On the other hand, as Figure 6 shows, even with computed intensities it is seen that at the STO-3G level the assignment of bands in the experimental spectra is essentially hopeless.

This comparison of the theoretical IR spectra with the well-characterized spectra of ethylene oxide has shown that computed frequencies and intensities should aid in the interpretation of less well-characterized spectra of small molecules.

Acknowledgment. This work was supported by a grant (GM29375) from NIH to one of us (P.L.P.).

Registry No. Ethylene oxide, 75-21-8; tetradeuterioethylene oxide, 6552-57-4.

The Dynamics of the Photochemical Decarbonylation of 3-Cyclopentenone

Blake I. Sonobe, T. Rick Fletcher, and Robert N. Rosenfeld*

Contribution from the Department of Chemistry, University of California, Davis, California 95616. *Received January 6, 1984*

Abstract: 3-Cyclopentenone undergoes photofragmentation, yielding butadiene and CO. The dynamics of this reaction have been investigated by using the method of time-resolved CO laser absorption spectroscopy. Nascent CO product vibrational energy distributions are directly determined. Dissociation at 193 nm yields CO with $N_0:N_1:N_2:N_3:N_4 = 1.00:0.30:0.11:0.04:0.01$, dissociation at 249 nm yields CO with $N_0:N_1:N_2 = 1.00:0.24:0.03$, and dissociation at 308 nm yields CO with $N_0:N_1 = 1.00:0.02$. The experimental distributions are analyzed by comparing them with distributions calculated by using a statistical model. On this basis, we conclude that only the nonfixed energy of the transition state is available for partitioning among the products' vibrational degrees of freedom and that the products are vibrationally decoupled from one another in the exit channel. Potential energy is thus released in the exit channel primarily to the relative translational motion of the products.

Photofragmentation reactions are of interest in the study of elementary reaction dynamics, in part because reactant activation can be accomplished, in the absence of collisions, to a well-defined total energy. This situation greatly simplifies the interpretation of experimental data on product translational, rotational, and vibrational energy distributions so that rather complete pictures of the photodissociation chemisty of small molecular species, e.g., tri- or tetraatomics, have begun to emerge.[1] This is not, however, the case for larger polyatomic systems where the increased number of internal degrees of freedom can introduce additional mechanistic and dynamical possibilities. For example, nonradiative electronic relaxation often competes favorably with direct dissociation in large polyatomics. Similarly, intramolecular vibrational relaxation can be rapid relative to dissociation so that the observed reaction dynamics reflect (microcanonical) ensemble-averaged behavior rather than that of a single ro-vibronic level. Studies of the photofragmentation dynamics of polyatomic molecules can provide some insight as to when such effects are important. The distribution of available energy among dissociation products' various degrees of freedom can yield information on transition-state structure and exit channel effects[2] (i.e., how do the separating products interact with one another). In this paper, we describe recent work from our laboratory on the photofragmentation of 3-cyclopentenone, eq 1, in the gas phase.[3] Energy partitioning

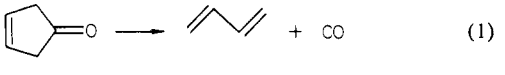

(1)

to the carbon monoxide product is probed by using the technique of time-resolved CO laser absorption spectroscopy. A physical model for the dissociation process is developed in terms of the shape of the reaction's potential surface.

The CO laser absorption method used here has been employed by other workers in studies of photodissociation dynamics.[4,5] Their results, in conjunction with those reported here, constitute a basis for developing detailed mechanistic/dynamical descriptions of elementary photofragmentation processes and provide bench-mark data with which the predictions of emerging ab initio techniques in dynamics may be compared.

Experimental Section

The instrumentation employed for CO laser absorption spectroscopy is illustrated schematically in Figure 1. 3-Cyclopentenone was slowly flowed through a 1-m absorption cell either neat at 0.08–0.5 torr or diluted in argon. Some care was taken to ensure that the reactant pressure was sufficiently low that a "thin target" approximation was valid. The absorption cell was equipped with CaF_2 windows mounted at Brewster's angle. The ketone was photoactivated with an excimer laser (Lambda Physik EMG 101; pulse width ca. 15 ns) using the XeCl*, KrF*, or ArF* transitions at 308, 249, or 193 nm, respectively. Laser fluences were typically 1–5 mJ/cm^2. The TEM_{00} output of a grating tuned, continuous wave (CW) CO laser was copropagated through the absorption cell coaxially with respect to the excimer laser. The CO laser was designed to optimize output on the ($1 \rightarrow 0$) vibrational transition,[6] where 5–8 mW could be routinely obtained. Appreciably more power was available when the laser was tuned to other vibrational transitions. The CO laser intensity transmitted through the absorption cell was monitored with a 2-mm diameter InSb detector. CO formed in the absorption cell by the photodissociation of 3-cyclopentenone produces a transient decrease in the CO laser intensity reaching the detector. The corresponding detector signal was amplified and then digitized with a Biomation 8100 transient recorder. The detection system rise time was $\lesssim$100 ns. The digitized signal was accumulated in a microcomputer for signal averaging. Typically, 500 transients were averaged. CO product vibrational distributions were determined by recording absorption curves with successive CO laser vibrational transitions until no further absorption could be detected. The CO laser grating drive was calibrated by using a 0.6-m monochromator to determine laser line wavelengths.

In all our experiments, sample pressures were measured with a capacitance manometer, and laser power or pulse energy was determined by using a Scientech power/energy meter. For each UV excitation wave-

(1) Leone, S. R. *Adv. Chem. Phys.* **1982**, *50*, 255.
(2) Polanyi, J. C. *Acc. Chem. Res.* **1972**, *5*, 161.
(3) Sonobe, B. I.; Fletcher, T. R.; Rosenfeld, R. N., submitted for publication in *Chem. Phys. Lett.*
(4) Houston, P. L.; Moore, C. B. *J. Chem. Phys.* **1976**, *65*, 757.
(5) Fujimoto, G. T.; Umstead, M. E.; Lin, M. C. *Chem. Phys.* **1982**, *65*, 197.
(6) Djeu, N. *Appl. Phys.* **1973**, *23*, 309.
(7) Siebert, D. R.; Grabiner, F. R.; Flynn, G. W. *J. Chem. Phys.* **1974**, *60*, 1564.

0002-7863/84/1506-4352$01.50/0

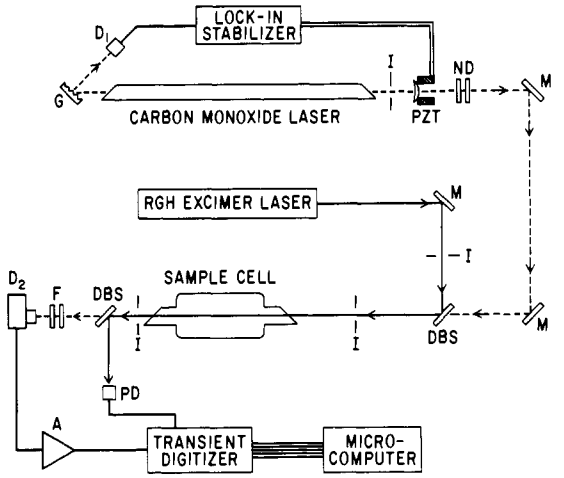

Figure 1. Diagram of experimental apparatus for time-resolved CO laser absorption spectroscopy. G, diffraction grating; I, variable iris; PZT, laser output coupler mounted on piezoelectric translator; D_1, PbSe detector; ND, neutral density filters; M, mirror; DBS, dichroic beamsplitter; PD, fast photodiode; F, infrared filters; D_2, InSb detector; A, amplifier.

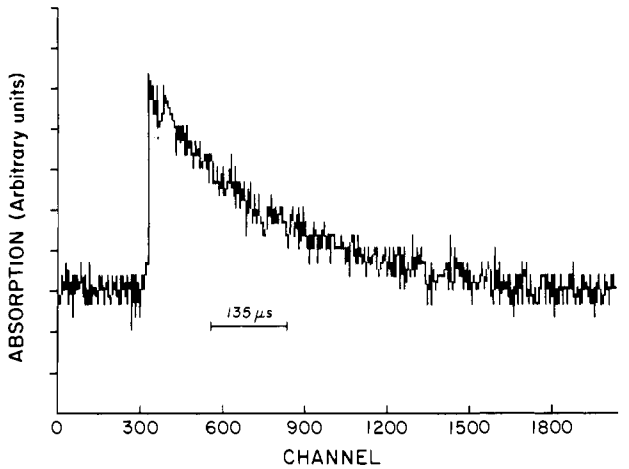

Figure 2. CO transient absorption curve obtained upon the photolysis of 0.5 torr of 3-cyclopentenone at 249 nm. The $P_{2,1}(9)$ CO laser transition was used as a probe. The reported curve was obtained by averaging 500 KrF* laser pulses.

length, a separate experiment was performed where the ketone was irradiated with ca. 1000 laser pulses. The products were subsequently analyzed by IR absorption spectroscopy.

Results

The photodissociation of 3-cyclopentenone results in the formation of carbon monoxide in some distribution of ro-vibrational states, $\{CO(v,J)\}$. A particular CO laser line, $P_{v+1,v}(J)$, will be resonantly absorbed by $CO(v,J)$. The initial, or rising, portion of the resulting transient asorption curve provides information on the *net* rate of formation of $CO(v,J)$, while the decaying portion of the curve is determined by the *net* relaxation rate of $CO(v,J)$. A typical transient absorption curve is shown in Figure 2. The maximum absorption amplitude for such curves provides a measure of the relative population of $CO(v)$, N_v, so long as negligible relaxation has occurred at the time that the amplitude measurement is made. For all of the cases discussed here, the absorption rise times were at least 10 times faster than the corresponding decay times; thus any relaxation processes can have only a minimal influence on the absorption maxima. Under these conditions, the N_v can be determined from maximum absorption amplitudes,[4] S_{v+1}, observed by using the $P_{v+1,v}(J)$ laser line as shown in eq 2. Here, v_m is the CO vibrational level beyond which

$$N_v \propto \sum_{i=v}^{v_m} \left(\frac{2J+1}{2J-1}\right)^i \frac{S_{i+1}}{i+1} \qquad (2)$$

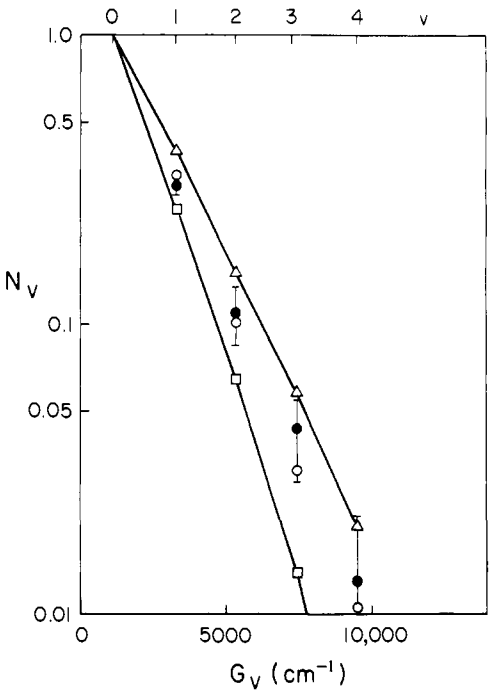

Figure 3. Nascent CO vibrational distribution from the 193-nm photolysis of 3-cyclopentenone. G_v is the CO vibrational term: (●), experimental data; (△, ○, and □) calculated by using eq 4 with an available energy E = 130, 100, and 80 kcal/mol, respectively.

no absorption signal can be observed; i.e., $N_v \approx 0$ for $v > v_m$. In our experiments, v_m is determined by signal/noise (rather than thermochemistry) which in turn is determined primarily by the amplitude stability of the CO and excimer lasers.

For all the excitation wavelengths investigated here, the effect of an inert buffer gas, argon, on absorption rise and decay times was examined. In every case, the addition of argon was found to *decrease* the absorption rise times and the absorption decay times. The effect of UV laser intensity on CO laser absorption amplitude was also investigated for each excitation wavelength. In all cases, absorption amplitudes were found to vary linearly with UV laser intensity. This indicates that CO is formed via single photon absorption in our experiments.

Thermal lensing effects could be observed in our experiments on a ca. 100-μs time scale at higher sample pressures. These lensing signals were easily differentiated from true absorption signals by their temporal behavior and by the observation that their amplitude was independent of the CO laser line employed; in fact, lensing could be observed by using CO laser lines, $P_{v+1,v}(J)$, for which $v > v_m$. Such effects were negligible at low sample pressures, and all quantitative work was done under low-pressure conditions.

Vibrational distributions for carbon monoxide produced by the photodissociation of 3-cyclopentanone were determined at three excitation wavelengths: 193, 249, and 308 nm. The results, shown in Figures 3–5, were obtained by using eq 2 to reduce the raw absorption data.

Irradiations of 3-cyclopetenone at 193, 249, and 308 nm were carried out and the products collected and analyzed by gas-phase infrared absorption spectroscopy. In all cases, the only products observed were carbon monoxide and 1,3-butadiene.

Discussion

Hess and Pitts[8] have studied the gas-phase photochemistry of 3-cyclopentenone at 3130 Å. They report that butadiene and CO are formed with quantum yields approaching unity. Triplet-sensitized photolysis[9] and pyrolysis[10] also yield these products

(8) Hess, L. D.; Pitts, J. N., Jr. *J. Am. Chem. Soc.* **1967**, *89*, 1973.
(9) Nakamura, K.; Koda, S.; Akita, K. *Bull. Chem. Soc. Jpn.* **1978**, *51*, 1665.
(10) Dolbier, W. R., Jr.; Frey, H. M. *J. Chem. Soc.*, Perkin *Trans 2* **1974**, 1674.

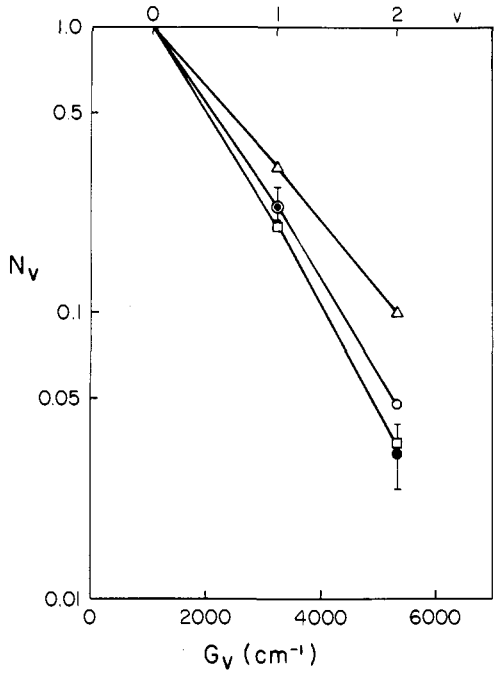

Figure 4. Nascent CO vibrational distribution from the 249-nm photolysis of 3-cyclopentenone: (●) experimental data, (△, ○, and □) calculated by using eq 4 with an available energy E = 100, 70, and 60 kcal/mol, respectively.

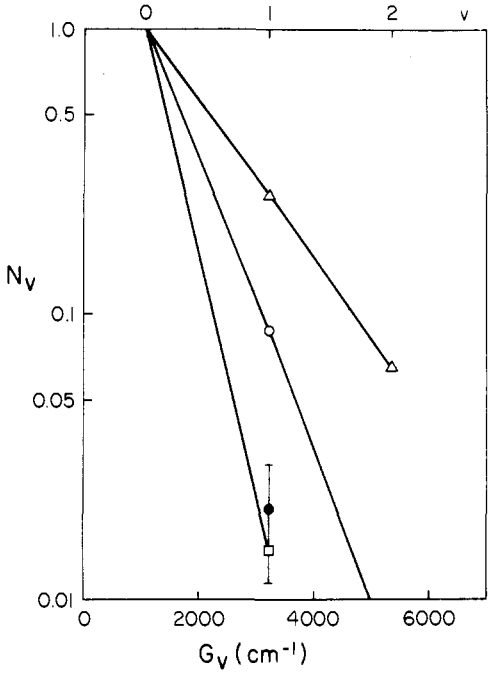

Figure 5. Nascent CO vibrational distribution from the 308-nm photolysis of 3-cyclopentenone: (●) experimental data, (△, ○, and □), calculated by using eq 4 with an available energy E = 80, 30, and 10 kcal/mol, respectively.

quantitatively. The reported[10] Arrhenius activation energy for (1) is ca. 57 kcal/mol, a value sufficiently low that the intervention of a biradical intermediate on the ground-electronic-state potential surface for dissociation, e.g., eq 3, can be ruled out. This follows

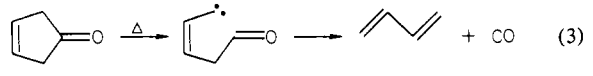

(3)

since thermochemical estimation methods[11] indicate an activation energy for (3) of at least 60 kcal/mol. It can therefore be concluded that eq 1 is a concerted process. Similar conclusions have been reached regarding the photochemical decarbonylation as a result of studies on stereochemically labeled 3-cyclopentenones.[12]

If the photofragmentation of 3-cyclopentenone occurs with spin conservation, insufficient energy is available to form electronically excited products for $\lambda \gtrsim 200$ nm. We thus suggest that nonradiative decay to the ground-state potential surface occurs prior to product formation in our experiments where $\lambda \geq 193$ nm. Nonradiative processes may be particularly facile in polyatomic molecules where low-frequency torsional and/or bending moles can serve to dramatically increase rovibrational state densities.[13] It is therefore reasonable to regard the dissociation of 3-cyclopentenone in analogy to a chemically activated unimolecular process. In this context, variation of the photoexcitation wavelength is equivalent to a concomitant variation in reactant internal energy.

The rise times of transient absorption curves, e.g., Figure 2, provide a qualitative indication of the extent of rotational excitation in the CO product. For all excitation wavelengths examined, CO absorption rise times are pressure dependent with $p\tau$'s of ca. 3×10^{-7} torr s. If the CO product was formed in a thermalized (300 K) distribution of rotational states, the absorption rise time would be detector limited, $\lesssim 1 \times 10^{-7}$ s, independent of pressure. Therefore, the CO formed by the photofragmentation of 3-cyclopentenone has a rotational temperature, T_r, $\gtrsim 300$ K (assuming a Boltzmann distribution of product rotational states). We have previously shown[14,15] that CO formed by the photodissociation of ketene at 193 nm has a rotational temperature $T_r \gtrsim 6700$ K. The corresponding CO absorption rise time, as determined by CO laser absorption spectroscopy,[16] is ca. 3×10^{-6} torr s. It is apparent that the photolysis of 3-cyclopentenone yields CO which is substantially colder, rotationally, than that obtained from ketene. However, a CO product rotational temperature cannot be determined from the present absorption data because of the limited tunability of our CO laser. The CO laser absorption *decay* times are determined by vibrational relaxation rates. In all cases, these decay times are at least 10 times slower than the associated absorption rise times. Under these conditions, the relative CO product *vibrational* populations, $\{N_v\}$, determined by eq 2, provide a good measure of the nascent CO product's vibrational distribution.[4]

The nascent vibrational distributions shown in Figures 3–5 can each be characterized by a vibrational temperature, T_v. This temperature is obtained from the slope of the best straight line through the data points of a N_v vs. G_v plot, where G_v is the CO vibrational term. For excitation wavelengths of 193, 249, and 308 nm, we find $T_v \simeq 2900$, 1800, and 640 K, respectively. This indicates that the extent of CO product vibrational excitation increases with photon energy or available energy (vide supra). Somewhat more insight regarding the physical significance of the experimentally determined vibrational distributions can be obtained by comparing these to the distributions anticipated on the basis of a model for energy partitioning among the products of a fragmentation reaction. For this purpose, we use a simple statistical model for energy disposal that has previously been described.[3,17,18] This model yields a CO vibrational energy distribution, f(*E*,E), for any specified available energy, E, eq 4.

$$f(E,\mathrm{E}) = \frac{N_{\mathrm{CO}}(E) \int_{\mathrm{E_t}=0}^{\mathrm{E}-E} P_r(\mathrm{E} - E - \mathrm{E_t}) E_t^{1/2} d\mathrm{E_t}}{\sum_{E=0}^{\mathrm{E}} N_{\mathrm{CO}}(\mathrm{E}) \int_{E_t=0}^{\mathrm{E}-E} P_r(E - E - \mathrm{E_t}) E_t^{1/2} d\mathrm{E_t}} \quad (4)$$

(11) Benson, S. W. "Thermochemical Kinetics", 2nd ed.; Wiley: New York, 1974.

(12) Darling, T. R.; Pouliquen, J.; Turro, N. J. *J. Am. Chem. Soc.* **1974**, *96*, 1247.
(13) Jortner, J.; Rice, S. A.; Hochstrasser, R. M. *Adv. Photochem.* **1969**, *7*, 149.
(14) Rosenfeld, R. N.; Sonobe, B. I. *J. Am. Chem. Soc.* **1983**, *105*, 1661.
(15) Sonobe, B. I.; Rosenfeld, R. N. *J. Am. Chem. Soc.* **1983**, *105*, 7528.
(16) Sonobe, B. I., unpublished results.
(17) Rosenfeld, R. N.; Weiner, B. *J. Am. Chem. Soc.* **1983**, *105*, 3485.
(18) Bogan, D. J.; Setser, D. W. *J. Chem. Phys.* **1976**, *64*, 586.

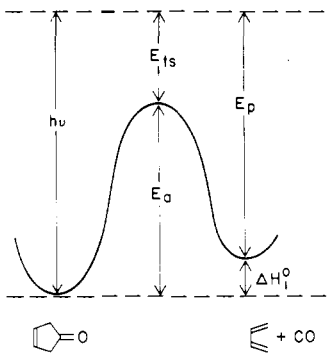

Figure 6. Schematic potential energy diagram for the dissociation of 3-cyclopentenone. E_p and E_{ts} correspond to the reaction exoergicity and the transition state's nonfixed energy, respectively.

Here $N_{CO}(E)$ is the CO vibrational density of states at energy E, $P_r(E)$ is the degeneracy of butadiene vibrational states and all relative rotational states at energy E, and $E_t^{1/2}$ is the one-dimensional translational-state density[19] at translational energy E_t. CO vibrational-state densities are computed from the harmonic oscillator approximation, and $P_r(E)$ is evaluated by using the Whitten–Rabinovitch semiclassical algorithm.[20] The statistical model, (4), allows us to compute CO product vibrational energy distributions under conditions where all product (CO and butadiene) modes are strongly coupled and the available energy is E. In this context, "strong coupling" means that intra- and interfragment V–V is facile on the time scale of the dissociation process.

CO vibrational distributions calculated by using eq 4 are plotted in Figures 3–5 for several choices of available energy. As a plausible a priori assumption, we might take the available energy to be determined by the reaction exoergicity, i.e., $E = h\nu - \Delta H°_1$ where $h\nu$ is the photon energy and $\Delta H°_1$ is the enthalpy change for eq 1. Thermochemical estimation methods[11] indicate $\Delta H°_1$ (298 K) = 15 kcal/mol. Thus, the reaction exoergicity is 130, 100, and 80 kcal/mol at 193, 249, and 308 nm, respectively. It is apparent in Figures 3–5 that the experimentally determined CO product vibrational distributions are in each case substantially colder than the distributions calculated by assuming $E = h\nu - \Delta H°_1$. Thus, if energy is statistically distributed among the products' vibrational degrees of freedom, the available energy must be less than the reaction exoergicity. For the 193-nm photolysis of 3-cyclopentenone, we find that the calculated CO vibrational distribution is consistent with the experimentally determined distribution when an available energy $E \simeq 100$ kcal/mol is employed (see Figure 3). When lower values of the available energy are used, the calculated distribution is qualitatively colder than that found experimentally. It therefore appears that ca. 100 kcal/mol of energy is available to the decomposing complex at a point on the potential surface where vibrational energy disposal is determined. If vibrational energy partitioning occurs in the vicinity of the transition state for dissociation, then the available energy is $E \approx h\nu - E_a$; i.e., $E \approx 97$ kcal/mol. This corresponds to the "nonfixed" energy of the transition state, in RRKM terminology.[21] Comparison of calculated and experimental CO vibrational distributions thus suggests that vibrational energy partitioning occurs at the transition state for the reaction (see Figure 6). This hypothesis can be evaluated by examining the influence of reactant internal energy (i.e., excitation wavelength) on the CO product vibrational distribution. When 3-cyclopentenone is photoactivated at 249 nm, the reaction exoergicity ($h\nu - \Delta H°_1$) is ca. 100 kcal/mol. The results shown in Figure 4 demonstrate that the CO distribution calculated with E = 100 kcal/mol is signficantly hotter than the experimental distribution. In this case, an available energy of 60–70 kcal/mol is required to obtain qualitative agreement between the experimental and the statistical model distributions. This available energy is comparable to the transition state's nonfixed energy, $h\nu - E_a \approx 64$ kcal/mol. Again, a comparison of experimental results with those anticipated on the basis of a statistical model suggest that vibrational energy partitioning occurs at the fragmentation transition state. The CO product vibrational distribution obtained on photolyzing 3-cyclopentenone at 308 nm is shown in Figure 5. The observed distribution is substantially colder than the statistical distribution computed on the assumption that the full reaction exoergicity of 80 kcal/mol is available. In fact, the experimental distribution appears colder than that calculated on the assumption that the transition state's nonfixed energy ($h\nu - E_a \approx 30$ kcal/mol) is partitioned among the products. An available energy of ca. 10 kcal/mol is required to obtain agreement with the experimental result. This discrepancy arises primarily from the fact that the semiclassical-state counting algorithm[20] we employ in evaluating eq 4 becomes a relatively poor approximation to direct count results at low energies.

Our results appear to validate the hypothesis that some energy less than the reaction exoergicity is available to the vibrational modes of the dissociation products of 3-cyclopentenone. If vibrational energy disposal occurs statistically, only the nonfixed energy of the transition state may be partitioned to the products' vibrational modes. This means that interfragment V–V becomes inefficient in the exit channel for the dissociation reaction. Since no evidence for extensive product *rotational* excitation was observed (compare to the case of ketene photodissociation),[14,15] the potential energy released in the exit channel, $E_a - \Delta H°_1$, must be partitioned primarily to the relative translational motion of the products. This conclusion is in accord with the results of recent molecular beam studies where product translational energy distributions are directly determined. For example, Lee and co-workers[22] have reported a study of the infrared multiphoton dissociation of ethyl vinyl ether which can decompose by two paths, one of which has a large activation barrier. Extensive translational energy release was observed only for the dissociation channel with the large barrier. Results have been reported by Setser and co-workers[23] on their studies of chemically activated haloalkane decomposition which further suggest the validity of this model. For these reactions, product vibrational energy distributions indicate that potential energy associated with the activation barrier is channeled preferentially to product translational motion. Lin and co-workers[5] have determined the vibrational energy distribution for the CO product formed by the dissociation of ketene at 193 nm. Ab initio calculations[24] indicate that this fragmentation has a negligible potential barrier (in excess of the reaction's endothermicity). Thus, the model described here suggests that the CO product vibrational energy distribution should be statistical, assuming the full reaction exoergicity to be available. This was, in fact, observed to be the case.[5]

Our results with 3-cyclopentenone indicate that energy disposal measurements can provide a useful probe of the photodissociation dynamics of polyatomic molecules. In particular, information on the interaction of nascent product fragments in the exit channel and near the transition state for dissociation can be obtained. We are currently examining the photofragmentation of some other cyclic ketones so that the influence of barrier height on energy disposal dynamics can be investigated more systematically.

Conclusions

Time-resolved CO laser absorption spectroscopy has been used to determine the nascent vibrational distribution of the CO product from the photolysis of 3-cyclopentenone at 193, 249, and 308 nm. The measured vibrational distributions were compared to those calculated by use of a statistical model. In this way, we find that only the nonfixed energy of the transition state is statistically

(19) Kinsey, J. L. *J. Chem. Phys.* **1971**, *54*, 1206.
(20) Whitten, G. Z.; Rabinovitch, B. S. *J. Chem. Phys.* **1964**, *41*, 1883.
(21) Robinson, P. J.; Holbrook, K. A. "Unimolecular Reactions"; Wiley-Interscience: New York, 1972.
(22) Huisken, F.; Krajnovich, D.; Zhang, Z.; Shen, Y. R.; Lee, Y. T. *J. Chem. Phys.* **1983**, *78*, 3806.
(23) Holmes, B. E.; Setser, D. W. "Physical Chemistry of Fast Reactions"; Plenum Press: New York, 1980; Vol. 2, p 83.
(24) Yamabe, S.; Morokuma, K. *J. Am. Chem. Soc.* **1978**, *100*, 7551.

partitioned among the products' vibrational modes; i.e., the full reaction exoergicity is not available for vibrational excitation of the fragments. Thus, as the transition state is transformed to products, the fragments are vibrationally decoupled from one another. The potential energy associated with the activation barrier is channeled principally to the relative translational motion of the products.

Acknowledgement is made to the donors of the Petroleum Research Fund, administered by the American Chemical Society, for partial support of this work. In addition, support for this work was provided by a grant from the National Science Foundation (NSF CHE-8206897).

Registry No. 3-Cyclopentenone, 14320-37-7.

Kinetics of Polyatomic Free Radicals Produced by Laser Photolysis. 3. Reaction of Vinyl Radicals with Molecular Oxygen

Irene R. Slagle, Jong-Yoon Park, Michael C. Heaven, and David Gutman*

Contribution from the Department of Chemistry, Illinois Institute of Technology, Chicago, Illinois 60616. *Received December 19, 1983*

Abstract: The kinetics and mechanism of the gaseous reaction of vinyl radicals with molecular oxygen have been studied between 297 and 602 K. The radicals were produced in a heated tubular reactor by the pulsed laser photolysis of C_2H_3Br at 193 nm. Reactant and product concentrations were monitored in real-time experiments using photoionization mass spectrometry. The products formed in this temperature range are HCO and H_2CO. The overall rate constant is pressure independent and is nearly constant with temperature: $k = 6.6\ (\pm 1.3) \times 10^{-12} \exp(250 \pm 100\ \text{cal}/RT)$ cm^3 molecule^{-1} s^{-1}. The magnitude of the rate constant, its temperature and pressure dependence, and the identity of the products of this reaction indicate that it proceeds by an addition mechanism in which the adduct rapidly rearranges to form an energy-rich dioxetanyl intermediate which decomposes into the observed products. Two other reactions (C_2H_3 + i-C_4H_{10} and C_3H_5 (allyl radical) + O_2) were investigated at elevated temperatures, but no reaction was detected. An upper limit (5×10^{-14} cm^3 molecule^{-1} s^{-1}) was established for the rate constants of both C_2H_3 + i-C_4H_{10} at 600 K and C_3H_5 + O_2 at 900 K.

Unsaturated hydrocarbon free radicals such as alkenyl and alkynyl radicals are particularly important intermediates in combustion processes.[1-3] These energy-rich hydrogen-deficient reaction intermediates are formed by the reactions of alkenes and alkynes with atoms and free radicals (such as H and OH),[4-6] and they subsequently react in two fundamentally different ways. They may react with molecular oxygen in extremely exothermic reactions that lead to stable oxygen-containing products or they may continue to lose hydrogen atoms in endothermic pyrolysis reactions that ultimately result in the production of soot precursors such as C_2H and C_3H_2.[5-9] A complete understanding of the kinetics and mechanisms of these two competing processes is essential for the quantitative modeling of macroscopic combustion phenomena such as soot formation and for the prediction of stable product yields.

A considerable amount of information is available on the thermal decomposition of free radicals based on experimental studies,[7,10-14] on additional investigations of the reverse reactions and the appropriate equilibrium constants,[15] and on estimates based on theoretical and thermochemical considerations.[16,17] Virtually nothing is known about the mechanisms or the rates of the reactions of unsaturated hydrocarbon free radicals with molecular oxygen. Only one has ever been isolated for direct study (C_2H + O_2),[18,19] and there is only one report of an indirect investigation of their mechanisms.[4] We have begun a series of studies of the reactions of unsaturated free radicals that are important in combustion processes. The first has involved the kinetics and mechanism of the C_2H_3 + O_2 reaction. This elementary reaction has never been isolated for direct study before, and there is no knowledge of its rate constant parameters. The results of this investigation are reported here.

Current kinetic models of combustion processes presume that the mechanism of the vinyl-radical reaction with O_2 at high temperatures is[5,7,9]

$$C_2H_3 + O_2 \rightarrow C_2H_2 + HO_2 \qquad \Delta H = -7\ \text{kcal} \qquad (1)$$

The use of this mechanism is based on the presumption that the C_2H_3 + O_2 reaction proceeds analogously to the C_2H_5 + O_2 reaction,[20] which is known to proceed by H-atom transfer to O_2

(1) Pollard, R. T. In "Comprehensive Chemical Kinetics"; Bamford, C. H., Tipper, C. F. H., Eds.; Elsevier: New York, 1977; Vol. 17, Chapter 2.
(2) Gardiner, W. C., Jr. *Sci. Am.* **1982**, *246*, 110.
(3) Warnatz, J.; Bockhorn, H.; Moser, A.; Wenz, H. W. *Symp. (Int.) Combust. [Proc.]* **1983**, *19*, 197-209.
(4) Baldwin, R. R.; Walker, R. W. *Symp. (Int.) Combust. [Proc.]* **1981**, *18*, 819-829.
(5) Westbrook, C. K.; Dryer, F. L.; Schug, K. P. *Combust. Flame* **1983**, *52*, 299-313.
(6) Homann, K. H.; Wellmann, Ch. *Ber. Bunsenges. Phys. Chem.* **1983**, *87*, 609-616.
(7) Warnatz, J. Report SAND83-8606; Sandia: Livermore, CA, Feb 1983.
(8) Westbrook, C. K.; Dryer, F. L. Report UCRL-88651; Lawrence Livermore National Laboratory: Livermore, CA, Feb 1983.
(9) Miller, J. A.; Mitchell, R. E.; Smooke, M. D.; Kee, R. J. *Symp. (Int.) Combust. [Proc.]* **1983**, *19*, 181-196.
(10) Walker, R. W. In "Gas Kinetics and Energy Transfer"; Ashmore, P. G., Donovan, R. J., Eds.; Chemical Society: London, 1977; Vol. 2, Chapter 7.
(11) Jachimowski, C. *J. Combust. Flame* **1977**, *29*, 55.
(12) Roth, P.; Barner, U.; Lohr, R. *Ber. Bunsenges. Phys. Chem.* **1979**, *83*, 929-932.
(13) Benson, S. W.; Haugen, G. R. *J. Phys. Chem.* **1967**, *71*, 1735-1746.
(14) Leathard, D. A.; Purnell, J. H. *Ann. Rev. Phys. Chem.* **1970**, *21*, 197.
(15) Payne, W. A.; Stief, L. J. *J. Chem. Phys.* **1976**, *64*, 1150.
(16) Choo, K. Y.; Benson, S. W. *Int. J. Chem. Kinet.* **1981**, *13*, 833.
(17) Burcat, A.; Skinner, G. B.; Grossley, R. W.; Scheller, K. *Int. J. Chem. Kinet.* **1973**, *5*, 345.
(18) Lange, W.; Wagner, H. Gg. *Ber. Bunsenges. Phys. Chem.* **1975**, *79*, 165-170.
(19) Laufer, A. H.; Lechleider, R. *J. Phys. Chem.* **1984**, *88*, 66-68.

0002-7863/84/1506-4356$01.50/0